NBS TECHNICAL NOTE 1031

U.S. DEPARTMENT OF COMMERCE /National Bureau of Standards

The Use of LEDs to Simulate Weak Yag-Laser Beams

NATIONAL BUREAU OF STANDARDS

The National Bureau of Standards[1] was established by an act of Congress on March 3, 1901. The Bureau's overall goal is to strengthen and advance the Nation's science and technology and facilitate their effective application for public benefit. To this end, the Bureau conducts research and provides: (1) a basis for the Nation's physical measurement system, (2) scientific and technological services for industry and government, (3) a technical basis for equity in trade, and (4) technical services to promote public safety. The Bureau's technical work is performed by the National Measurement Laboratory, the National Engineering Laboratory, and the Institute for Computer Sciences and Technology.

THE NATIONAL MEASUREMENT LABORATORY provides the national system of physical and chemical and materials measurement; coordinates the system with measurement systems of other nations and furnishes essential services leading to accurate and uniform physical and chemical measurement throughout the Nation's scientific community, industry, and commerce; conducts materials research leading to improved methods of measurement, standards, and data on the properties of materials needed by industry, commerce, educational institutions, and Government; provides advisory and research services to other Government agencies; develops, produces, and distributes Standard Reference Materials; and provides calibration services. The Laboratory consists of the following centers:

Absolute Physical Quantities[2] — Radiation Research — Thermodynamics and Molecular Science — Analytical Chemistry — Materials Science.

THE NATIONAL ENGINEERING LABORATORY provides technology and technical services to the public and private sectors to address national needs and to solve national problems; conducts research in engineering and applied science in support of these efforts; builds and maintains competence in the necessary disciplines required to carry out this research and technical service; develops engineering data and measurement capabilities; provides engineering measurement traceability services; develops test methods and proposes engineering standards and code changes; develops and proposes new engineering practices; and develops and improves mechanisms to transfer results of its research to the ultimate user. The Laboratory consists of the following centers:

Applied Mathematics — Electronics and Electrical Engineering[2] — Mechanical Engineering and Process Technology[2] — Building Technology — Fire Research — Consumer Product Technology — Field Methods.

THE INSTITUTE FOR COMPUTER SCIENCES AND TECHNOLOGY conducts research and provides scientific and technical services to aid Federal agencies in the selection, acquisition, application, and use of computer technology to improve effectiveness and economy in Government operations in accordance with Public Law 89-306 (40 U.S.C. 759), relevant Executive Orders, and other directives; carries out this mission by managing the Federal Information Processing Standards Program, developing Federal ADP standards guidelines, and managing Federal participation in ADP voluntary standardization activities; provides scientific and technological advisory services and assistance to Federal agencies; and provides the technical foundation for computer-related policies of the Federal Government. The Institute consists of the following centers:

Programming Science and Technology — Computer Systems Engineering.

[1]Headquarters and Laboratories at Gaithersburg, MD, unless otherwise noted; mailing address Washington, DC 20234.
[2]Some divisions within the center are located at Boulder, CO 80303.

The Use of LEDs to Simulate Weak Yag-Laser Beams

M. Young

Electromagnetic Technology Division
National Engineering Laboratory
National Bureau of Standards
Boulder, Colorado 80303

U.S. DEPARTMENT OF COMMERCE, Philip M. Klutznick, Secretary
Jordan J. Baruch, Assistant Secretary for Productivity, Technology and Innovation
NATIONAL BUREAU OF STANDARDS, Ernest Ambler, Director

Issued January 1981

NATIONAL BUREAU OF STANDARDS TECHNICAL NOTE 1031

Nat. Bur. Stand. (U.S.), Tech. Note 1031, 48 pages (January 1981)

CODEN: NBTNAE

U.S. GOVERNMENT PRINTING OFFICE
WASHINGTON: 1981

For sale by the Superintendent of Documents, U.S. Government Printing Office, Washington, D.C. 20402

Price $2.50 (Add 25 percent for other than U.S. mailing)

CONTENTS

THE USE OF LEDs TO SIMULATE WEAK YAG-LASER BEAMS

M. Young

Electromagnetic Technology Division
National Engineering Laboratory
National Bureau of Standards
Boulder, Colorado 80303

Abstract

The purpose of this report is to determine whether and under what conditions a light-emitting diode may be used to simulate a weak YAG-laser beam that has been scattered by a distant reflecting object. By examining the differences between laser radiation and LED radiation, we conclude that there is no theoretical reason that a LED may not be used in place of the laser beam.

Key words: Laser simulator; light-emitting diodes; YAG laser.

THE USE OF LEDs TO SIMULATE WEAK YAG-LASER BEAMS

The purpose of this report is to determine the conditions under which a light-emitting diode (LED) may be used to simulate a weak laser pulse at the wavelength of 1064 nm. The pulse is presumed to have originated from the diffuse scattering of a laser beam off a distant object. We seek to determine the feasibility of testing the receiver of such a pulse with the suitably collimated and filtered radiation of a 1060-nm LED.

Much of the report is theoretical; the remainder is either experimental or supported by experimental evidence. Because of the organization of the document, theoretical and experimental considerations are not divided into separate sections; rather, we take the approach outlined below.

We begin by asking the question, What are the potential differences between laser radiation and LED radiation? The laser radiation in question is presumed to be Nd:YAG radiation that has been scattered from a distant object. The LED radiation is presumed to have originated from one of several (nominally) 1060-nm LEDs that are on the market.

To answer the question, we have compiled a list of parameters that will have to be examined. We have tried to make the list as exhaustive as possible, even though in some areas potential problems may be dismissed out of hand. The list is presented as Table 1. Other ways of organizing the list are possible; this organization best suits our needs.

Table 1.
Potential Areas of Difficulty

1. Wavelength.
   a. Wavelength of maximum power.
      i. Detector responsivity vs. wavelength.
   b. Linewidth.
      i. As it relates to a.
      ii. Coherence length.
   c. Chirping of LED.

2. Beam divergence.
    a. Degree of collimation of simulator, compared with laser return.
    b. Spatial coherence.
3. Pulse duration and shape.
4. Energy density over aperture.
    a. Uniformity over aperture.
    b. Pulse-to-pulse energy.

Apparatus and Procedures

Before going on to discuss the entries in Table 1 in detail, we must describe the experimental apparatus.

We obtained six LEDs whose wavelength was nominally 1060 nm. We excited the LEDs with a signal generator that could provide electrical pulses up to 2 A and as short as 20 ns. The circuit is shown in Fig. 1. The diode provides protection for the LED in case of a strong, negative reflection. The series resistor provides an impedance match to the 50-Ω coaxial cable; its value is chosen experimentally by time domain reflectometry.

A microwave tee with a 270-Ω resistor is used to sample the electrical pulse in the coaxial cable. We use enough cable between the LED and the generator to provide a 35-ns round-trip delay and operate the generator at the 20-ns setting. We use a sampling oscilloscope to observe the direct and reflected waveforms as they pass the tee. Following [1], we adjust the value of the series resistor until the waveform shows slight undershoot; when possible, we also ensure that none of the secondary oscillations becomes positive, because this will cause a small, secondary optical pulse. Figure 2 shows the effect of changing the series resistor on the electrical waveform of a particular LED.* The data were taken with the horizontal and vertical outputs of the sampling oscilloscope connected to an xy recorder; the vertical output was filtered with a capacitor to reduce noise (more on this later).

In principle, the effective impedance of the LED and of the diode are functions of peak current and waveform. However, we have found that slight

*The use of product names is intended for the convenience of the reader and does not imply endorsement by the National Bureau of Standards. Products of other manufacturers may work as well or better.

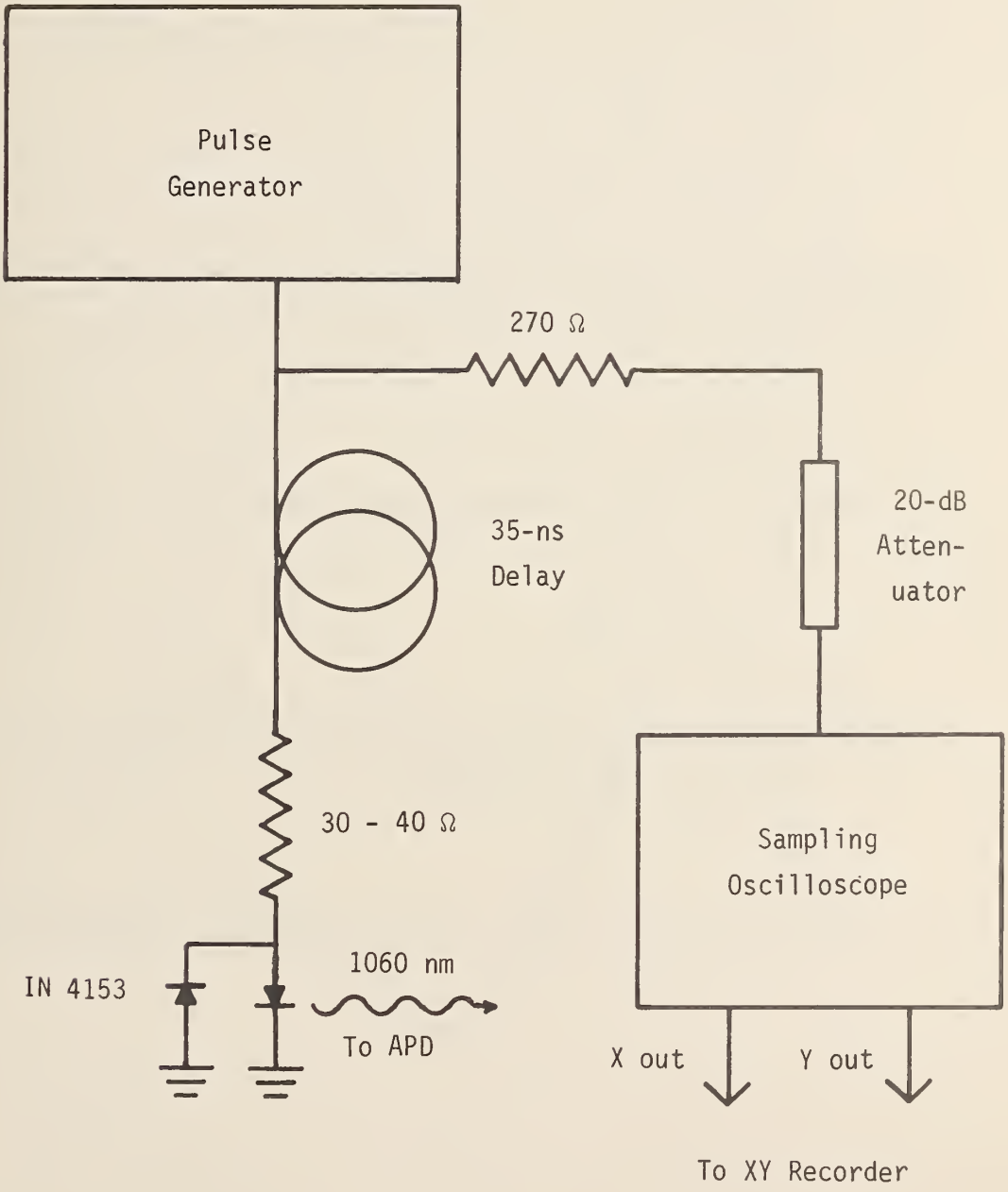

igure 1. Circuit for driving 1060-nm LED and monitoring direct and reflected current waveforms.

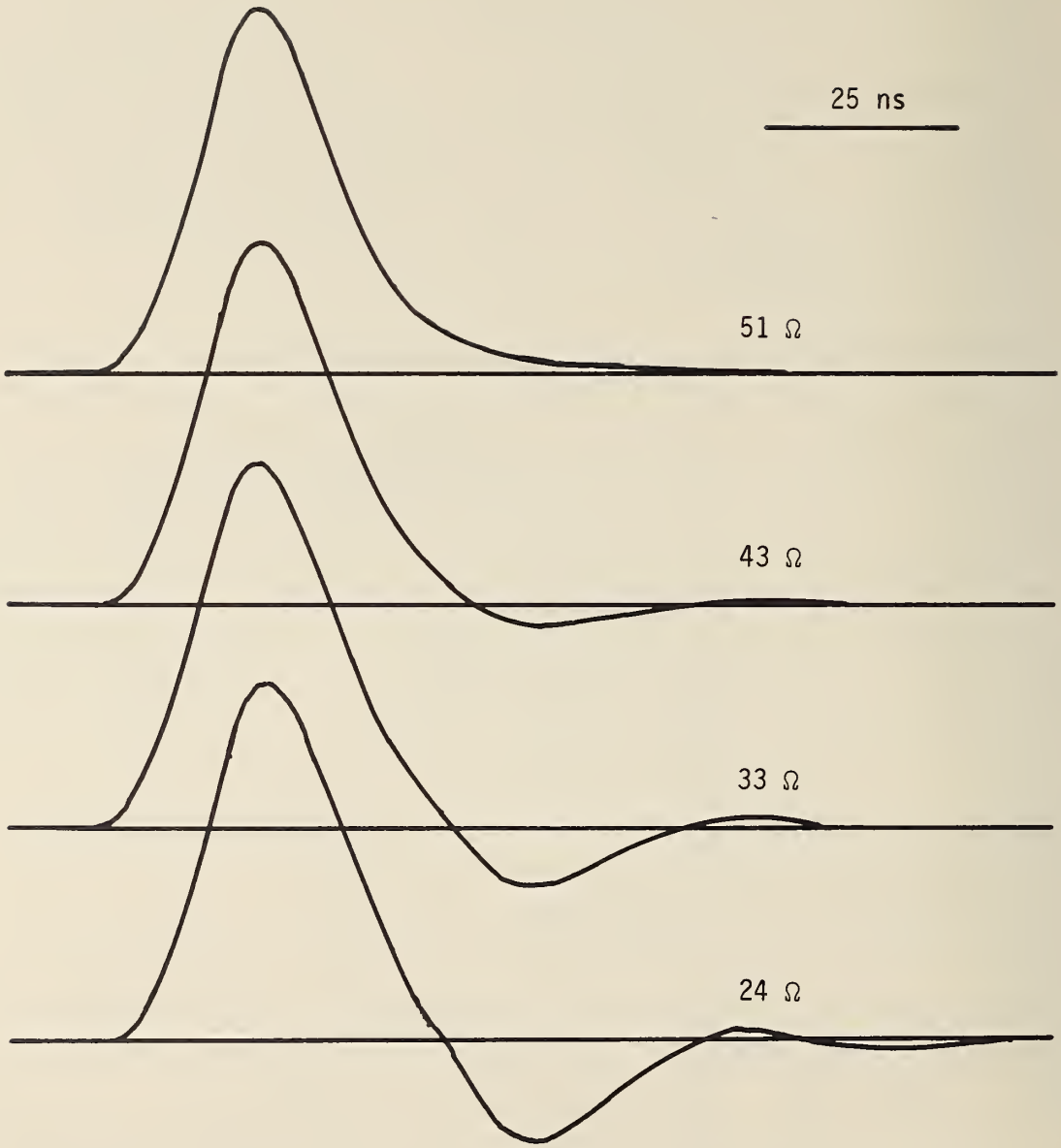

Figure 2a. Examination of direct and reflected current waveforms as function of series resistance.

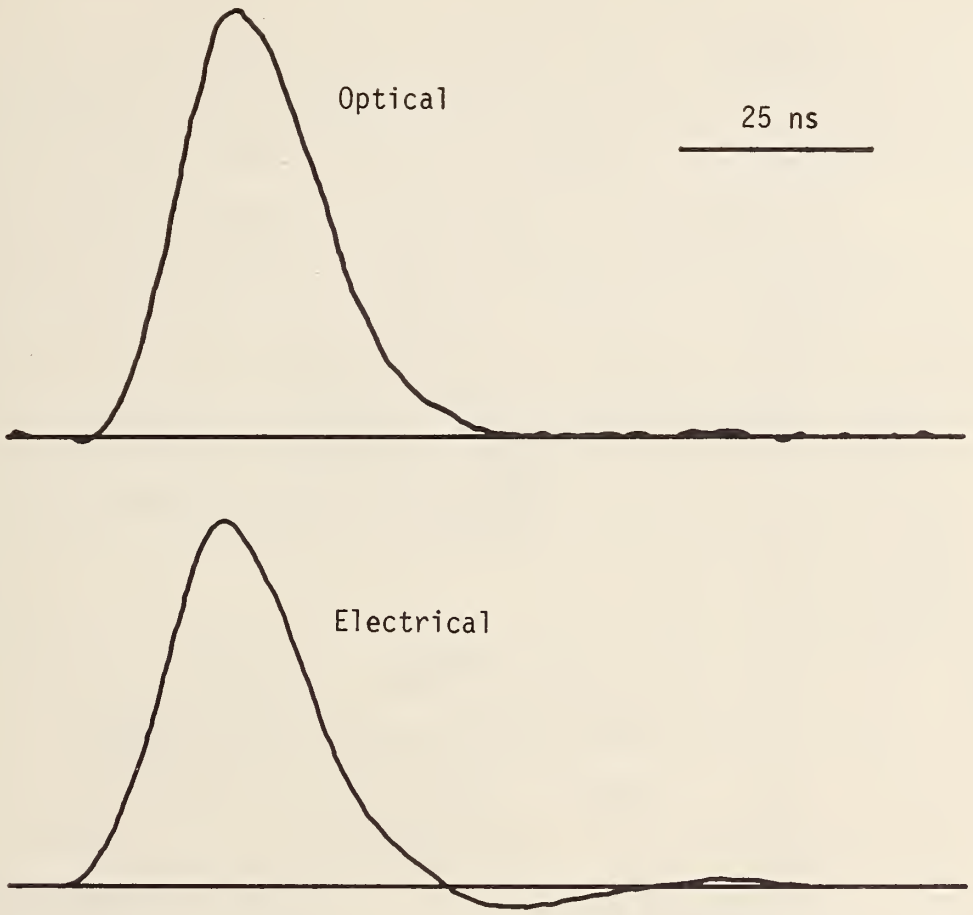

ure 2b. Optical pulse emitted when LED is driven by current waveform shown. Diode is a GAL 100, with a 43-Ω series resistor and approximately 1-A peak current.

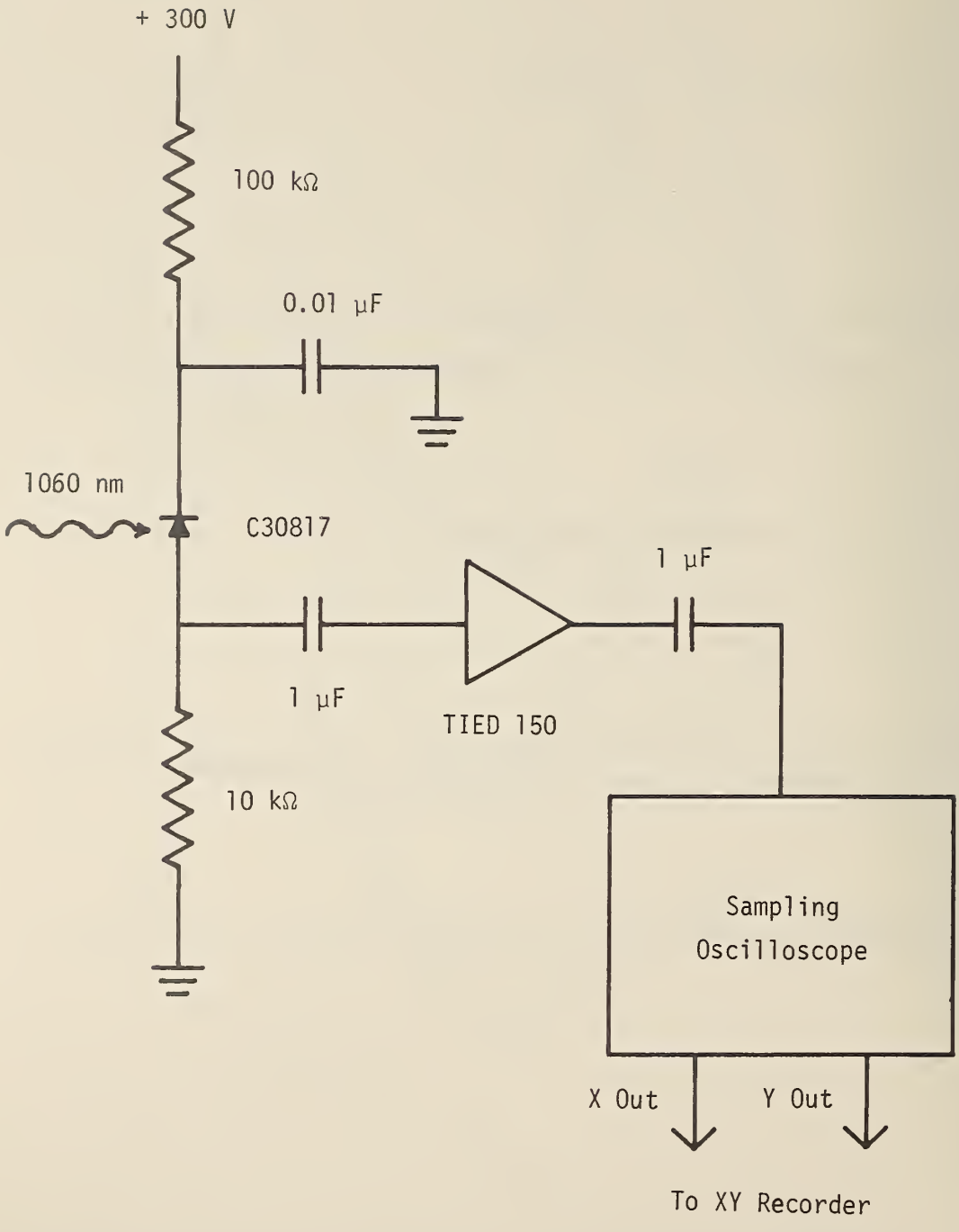

Figure 3. Avalanche photodiode and associated electronics.

changes of the peak current are not serious. We matched the impedance of the system at the peak current of 1 A but frequently operate satisfactorily at 2 A.

To detect the radiation, we use an avalanche photodiode, usually followed by a transimpedance amplifier and sometimes by a radio-frequency amplifier as well. The circuit is shown in Fig. 3. As before, the waveform is detected by the sampling oscilloscope and transcribed by the xy recorder.

For many experiments, we wanted to measure the optical power at a given time (such as the peak of the pulse) as a function of some parameter such as wavelength or source or detector position. For this purpose, we fashioned a mechanical-to-electrical transducer and used the transducer output to drive the horizontal motion of the xy recorder. For the vertical motion, we set the sampling oscilloscope on "manual" and set the display at a fixed time; we use the output of the oscilloscope to drive the vertical amplifier of the recorder.

The sampling oscilloscope displays about 5 mV of noise, peak to peak; when we use the rf amplifier, it adds another 5 mV of noise. Many times, this results in a signal-to-noise ratio no better than 3 or 5. In part to reduce the effect of this noise, we record our waveforms with the xy recorder instead of the more-common oscilloscope photography. By scanning sufficiently slowly and integrating with a capacitor, we perform an analog average of the noise and improve the signal-to-noise ratio by an order of magnitude or more.

We will describe further details of the experiments as we need them. The rest of the report is organized parallel to Table 1.

Wavelength

The YAG laser emits radiation at the wavelength of 1064 nm; its linewidth is of the order of 0.5 nm. The LEDs, on the other hand, display a peak wavelength in the neighborhood of 1060 nm and a linewidth of about 50 nm. In addition, the peak wavelength depends on temperature, so there is the possibility that the spectrum will drift during the course of the pulse (this is known as "chirping").

To assess these problems, we first calibrated a 1/4-meter grating monochromator with a continuous-wave YAG laser. We excited the LEDs with 2-A, 20-ns pulses and observed the spectrum at various times during the pulses.

For this purpose, we set the oscilloscope on "manual," as described above, and electrically connected the wavelength drive of the monochromator with the horizontal amplifier of the recorder.

Figure 4 shows some spectra obtained with one of the LEDs. In general, the wavelength of maximum radiance is not 1064 nm, but is more nearly 1050 in most cases. The linewidth and wavelength of maximum for all six LEDs are compiled in Table 2 and compared with the manufacturers' specifications.

Table 2.

Spectral Data on LEDs

	Wavelength of maximum (nm)		Linewidth (nm)		$P(1064)/P_{max}$	Power at 2-A drive (mW)
	spec	actual[3]	spec	actual		spec
C30116/F #1	1030-1090[1]	1047	60	45	0.72	4
C30116/F #3	" "	1045	"	42	0.56	"
GAL 100	1050-1065[2]	1050	55	50	0.85	
GAL 101 #1	1050-1065[2]	1042	"	51	0.57	4[4]
GAL 101 #2	" "	1045	"	52	0.73	"

[1] At 27°C
[2] At 25°C
[3] At 25°C
[4] Into F/1 cone

Let us assume for the moment that one of the LEDs is to be calibrated with an instrument that contains a silicon detector. The detector's responsivity has been calibrated with a YAG laser at the wavelength of 1064 nm. A check of several manufacturers' specifications shows that the responsivity of the detectors varies with wavelength by 1 to 2 percent per nanometer. Therefore, the calibration will be in error by about 10 percent if the maximum wavelength of the LED is in the range of 1050 to 1055 nm. Possibly this will not be a serious error.

More important, however, is the problem of using the LED with an instrument that contains a narrowband filter centered about 1064 nm. Let us assume that the filter has a bandwidth of 10 nm. The system is designed to detect radiation whose linewidth is substantially less than 10 nm; thus, to calibrate

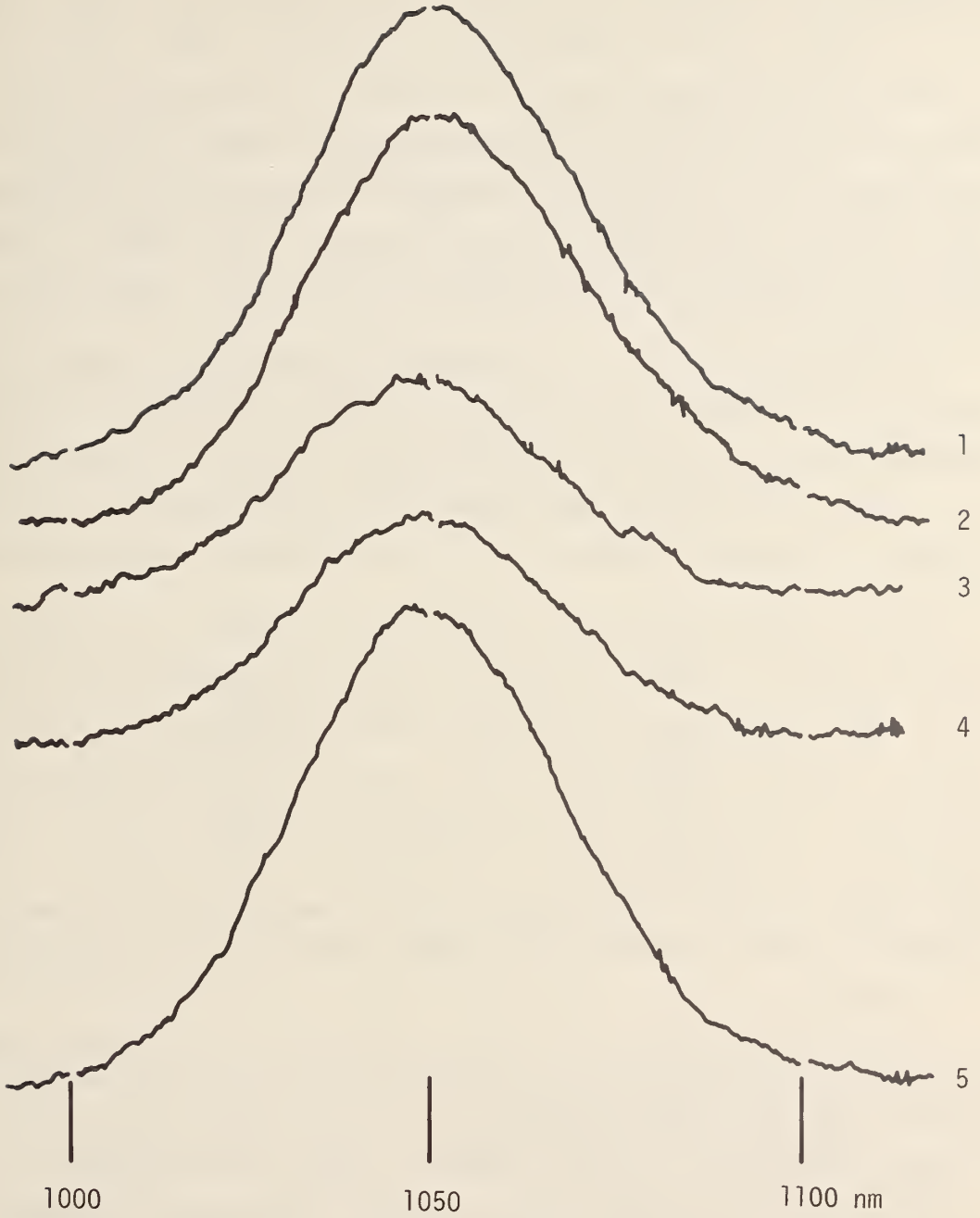

ure 4. Spectra of C30116/F #1. 1--beginning of 1-μs pulse; 2--end of 1-μs pulse; 3--second half-power point of 20-ns pulse; 4--first half-power point of 20-ns pulse; 5--peak of 20-ns pulse. Peak current was 2 A and repetition frequency was 1 kHz. Vertical scales are not necessarily the same.

the system directly with a LED, the LED will have to be filtered to 0.5 nm or so. Most of the radiation from the LED is therefore discarded (see Appendix A).

If the accuracy required is not too great, it may be desirable to use the LED unfiltered. Its spectrum must be measured and the transmittance through the receiver's filter calculated. Appendix A shows how to estimate this transmittance for the purpose of initial design. The estimate is reasonably accurate, provided that the linewidth of the LED greatly exceed the bandwidth of the filter.

A third approach is to filter the LED radiation with a filter that is identical to the filter inside the receiver. The calibration of the emitter is performed on the filtered radiation; there is no need to measure the spectrum. Twenty to fifty times more power will be available than with the narrowband filter, but the measurement of the receiver's responsivity must be performed with care.

Appendix A shows how to calculate the transmittance of a filter when the spectrum of the radiation is identical to the transmittance curve of the filter. When the spectrum can be approximated adequately by a Gaussian function, the overall transmittance of the filter is 0.35 times the maximum transmittance T_0. If the filters are not precisely identical or if the Gaussian approximation is inadequate, then the factor will differ from 0.35. The transmittance is not, in any case, T_0 and must be calculated correctly if the simulator is to be calibrated with a filter that is similar to the filter in the instrument.

In cases where energy is limited, we favor the last approach because it makes relatively efficient use of the total LED radiation and because the required calculation does not depend on a measurement of the spectrum of each LED. When energy is not limited, the narrow-band filter is appropriate.

The linewidth of a source also determines the temporal coherence of the radiation. The linewidth of the YAG laser is about 100 times less than that of the LED; its coherence length is therefore 100 times greater. It may be argued that the higher coherence of the laser will cause effects that will not be seen when the LED is used as a source.

The coherence length of a source is equal to $1/2\pi\Delta\nu$, where $\Delta\nu$ is the linewidth in the frequency domain [2]. The coherence length of the YAG laser is about 0.5 mm. There should be no problem resulting from coherence unless

the system contains two surfaces that are precisely parallel and well under a millimeter apart. The filtered LED radiation will display a greater linewidth than the laser; temporal coherence will therefore be less a factor.

Finally, we address the problem of chirping. Chirping could result from rapid heating of the diode during the current pulse (see Table 3). To determine whether the wavelength of maximum radiance shifts during the pulse, we recorded the spectra of several of the LEDs at different times during the pulse. For example, Fig. 4 shows the spectra at the first half-power point, the peak and the second half-power point of a 2-A, 20-ns pulse. Apart from power, the spectra are not distinguishable.

Table 3

Wavelength of "Typical" LED vs. Temperature*

Temperature (K)	Wavelength (nm)
120	1004
140	1009.5
160	1014
180	1019
300	1050

*These data and certain others courtesy of Rudy Garza, Plessey Optoelectronics and Microwave Ltd.

Further to ensure that chirping would not be a problem, we lengthened the pulses to 1 μs and measured the spectra at the beginning and end of the pulses. We thereby established an upper limit of ~ 1 nm/μs to the rate of wavelength drift of the LEDs (GAL 101s) with the highest current density. This is negligible compared with the ~ 50-nm spectral width of the source. We therefore conclude that chirping will not be a problem at least up to the peak current of 2 A. If the pulse duration is restricted to < 100 ns, we speculate that chirping will be negligible up to the maximum rated current of 10 A.

Beam Divergence

If a source is placed precisely at the focal point of a diffraction-limited lens, the beam refracted by the lens will be collimated but will still exhibit a small divergence. The divergence will result either from diffraction or from the finite size of the source. In either case, we refer to this residual divergence as "the beam divergence"; it is to be distinguished from the divergence of a beam that is not as well collimated as possible.

Beam divergence in the LED simulator is important if the receiver to be tested is spatially filtered to limit the field of view to a certain angle. If this is the case, then the LED radiation will have to be collimated and its beam divergence restricted to less than the field of view of the receiver.

To pursue this investigation further, we describe a "typical" system that will serve as a paradigm for all practical systems (see Table 4). Consider a laser transmitter that projects a beam with (full-angle) divergence 0.5 mrad onto a diffusely scattering object 10 km distant. The receiver that detects the scattered light is alongside the transmitter and is therefore also 10 km distant from the scatterer. (We do not discuss here whether or not the laser radiation can be detected in the presence of a daytime background.) A detector is located at the focal plane of the objective lens associated with the receiver.

Table 4
"Typical" System

Wavelength	1064 nm
Linewidth	0.5 nm
Beam divergence (full angle)	0.5 mrad
Energy per pulse	0.1 J
Duration	50 ns
Range	10 km
Receiver entrance pupil diameter	10 cm
Receiver linewidth	10 nm

Figure 5 shows the geometry. ℓ is the range and α is the divergence of the transmitter. The size of the spot projected onto the diffuser is

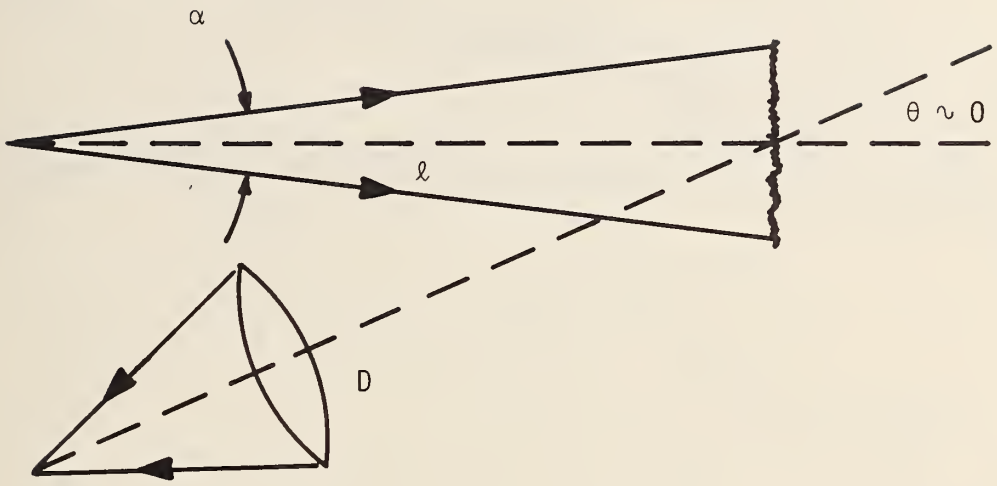

Figure 5. Geometry of laser beam scattered by distant diffuser.

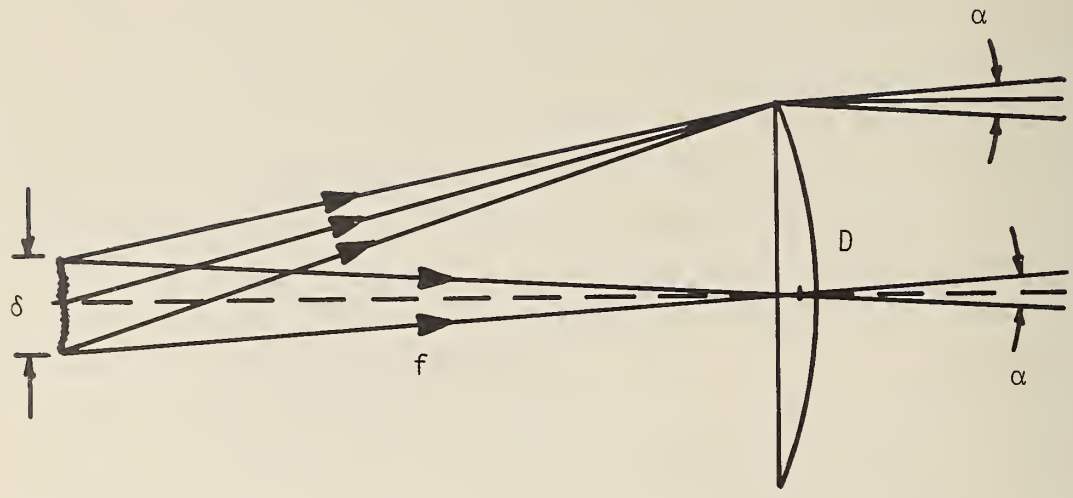

Figure 6. Divergence of beam collimated by lens with finite source.

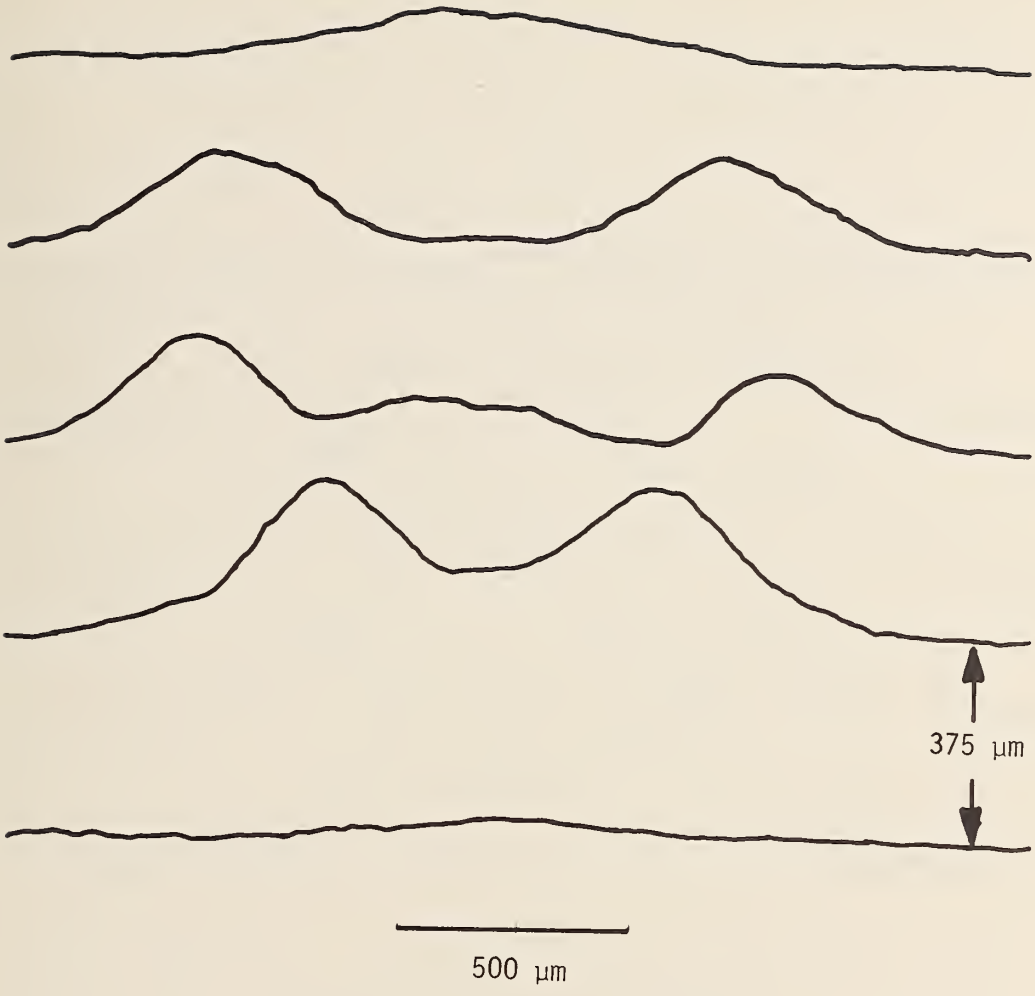

Figure 7a. Near-field scan of C30116/F #3.

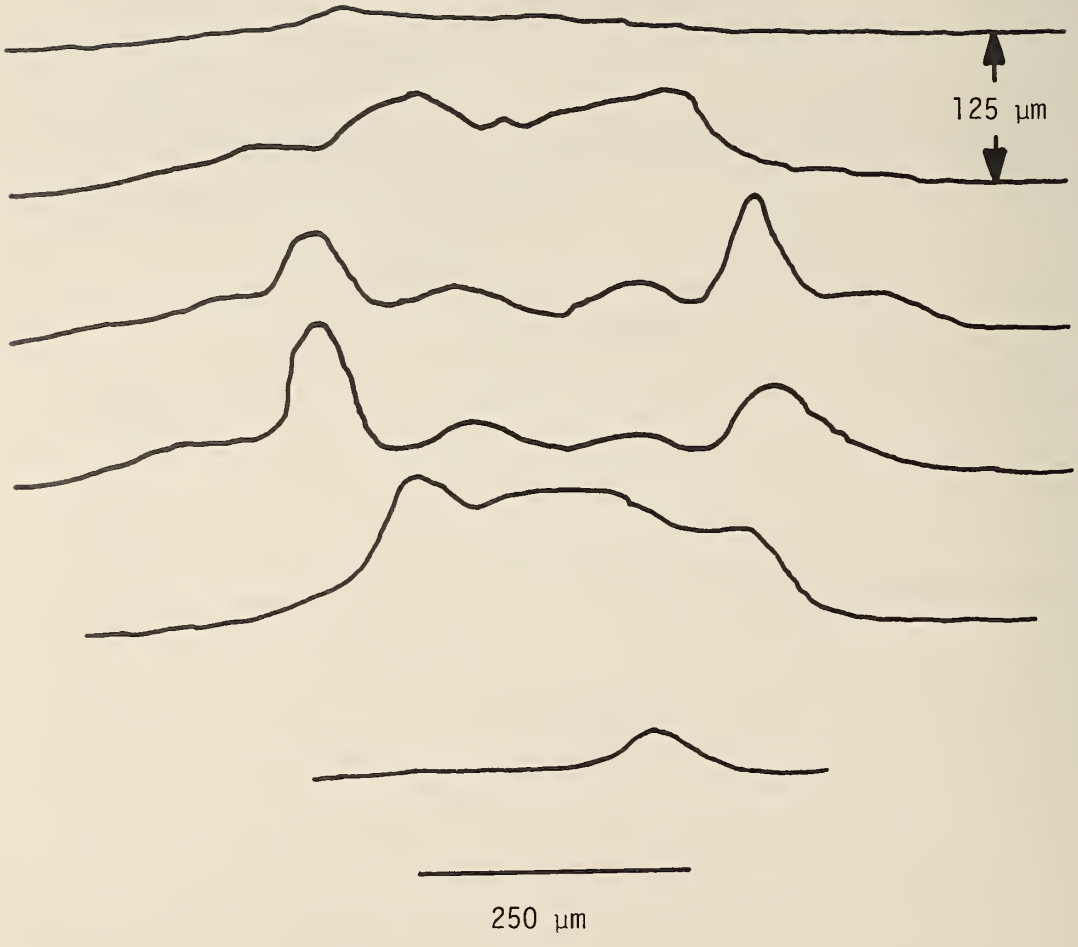

Figure 7b. Near-field scan of GAL 100.

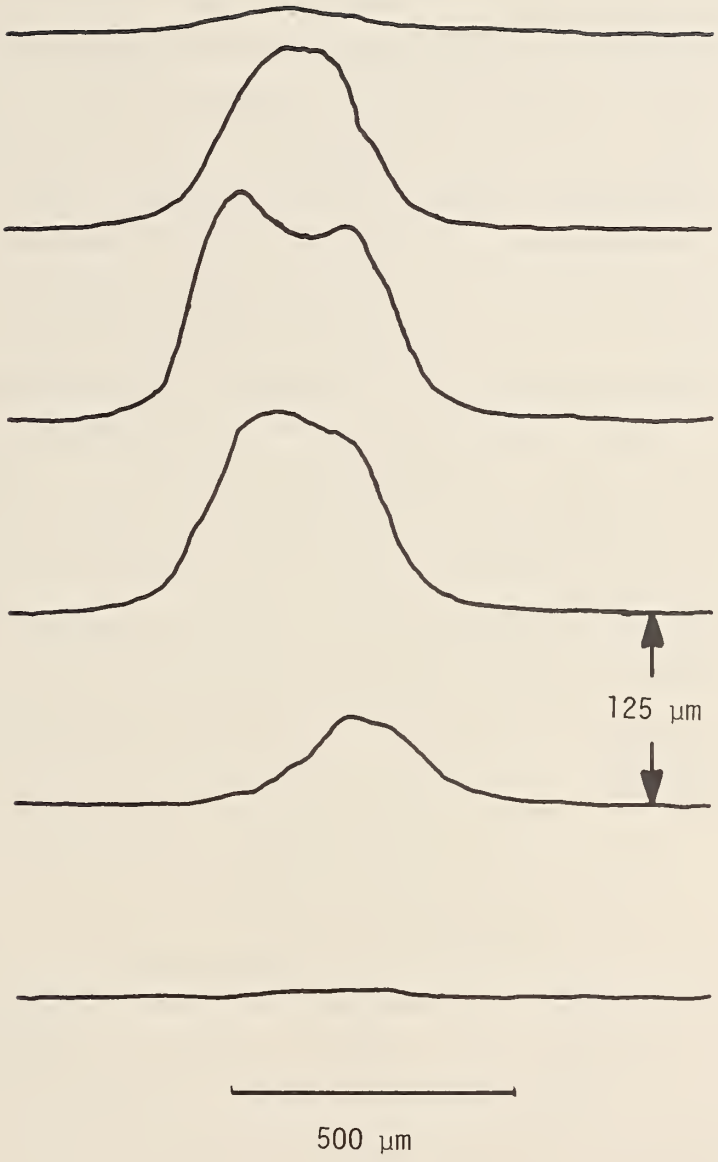

Figure 7c. Near-field scan of GAL 101 #2.

therefore $\ell\alpha$. To detect all the radiation scattered into its entrance pupil, the receiver must have a field of view at least equal to the diameter of the illuminated spot divided by the range. This is just equal to the divergence of the transmitter, or 0.5 mrad. We shall therefore require that the LED radiation be collimated and its divergence restricted to less than 0.5 mrad.

The beam divergence is determined from the geometry of the LED and the collimating lens or mirror. Figure 6 shows that the beam divergence is equal to the diameter of the LED divided by the focal length of the lens. For example, a 0.1-mm LED (such as a GAL 101) will give a beam divergence of 0.2 mrad when collimated by a 50-cm lens. In addition, Appendix B shows how to calculate the acceptable amount of focus error for given geometry.

The beam divergence is more easily calculated than measured directly. However, it is instructive to scan the near-field radiation pattern of the LEDs. We have performed this scan by fixing the LEDs to a translation stage. The stage is connected (with the position transducer) to the horizontal amplifier of the xy recorder. The image of the LED is projected with a 10X microscope objective onto the plane of a detector that is considerably smaller than the image. Figure 7 shows the results of some near-field scans; Table 5 relates the manufacturers' specifications with the measured diameters of the radiation patterns.

Table 5
Dimensions of LEDs

	Spec (μm)	Measured luminous diameter (μm)
C30116/F #1	450	1700
C30116/F #3	450	1600
GAL 100	400	400
GAL 101 #1	100	550*
GAL 101 #2	100	560*

*Apparent diameter, seen through ruby lens and thin layer of GaAs.

The C30116/Fs appear considerably larger than the manufacturer's claim. In addition, most of the radiation emanates from a ring around the outside of the pattern. We inspected the LEDs with a microscope and, through the microscope, with an infrared viewer. Although they are classified as surface emitters, they clearly emit a large fraction of their radiation through the edges of the chip; this radiation is reflected from the rounded sides of the well in which the chips appear to sit. Most of the radiation that reaches the outside appears to be such reflected radiation. This has the effect of making the effective source larger than the LED itself. (The manufacturer's specification evidently refers to the size of the chip.)

The GAL 101s likewise appear considerably larger than the 100-μm emitting area claimed by the manufacturer. According to the manufacturer, the junction of the LED lies 20-45 μm below the surface of the chip. A hemispherical ruby lens with ~ 400 μm diameter is contacted to the chip. This optical system produces a virtual image of the emitter at very nearly the location of the emitter. The magnification of this optical system is about 1.8 (see Appendix C); the scan reveals a source several times larger than 180 μm.

We examined these LEDs as well with the microscope and the infrared viewer. Our examination verified that the apparent source diameter is several times larger than the virtual image of the emitter (which could be seen as a small circular area behind the hemispherical lens). Because we do not know the structure in detail, we cannot account for the apparent size of the source.

The ruby lens probably increases the irradiance in the forward direction by roughly the amount estimated in Appendix C. However, the apparent radiance of the GAL 101s is substantially less than what would be calculated on the basis of a 180-μm emitter. If a source whose diameter is truly 100 μm is required, then it may be possible to obtain one by using this LED without the ruby lens. (We obtained one LED without the lens; it broke after being mounted and could not be replaced in time for this report.)

The nonuniformity of the near-field scans of the LEDs is acceptable, provided that the overall beam divergence be sufficiently small; that is, provided that the focal length of the lens times the acceptable beam divergence exceed the total luminous diameter of the LED. The nonuniform near field will not affect the uniformity of the beam across the surface of the collimating lens.

The beam divergence will be equal to that calculated provided that the collimating lens be sufficiently aberration free. The properties of the lens may be calculated by a ray trace if necessary; however, third-order aberration theory is sufficiently precise. When one conjugate is located at infinity, the optimum lens shape is very nearly planoconvex. Because planoconvex lenses are readily available, we restrict ourselves to this type. Appendix D shows how to calculate the third-order aberrations of a planoconvex lens oriented with the curved side toward the infinite conjugate. The lens will be diffraction limited if the overall aberration is less than the Airy-disk radius; it will display acceptable quality if the aberration is less than the size of the emitter. Further details are left to the appendix.

The size and range of the illuminated diffuser also influence the degree of spatial coherence of the radiation incident upon the receiver. If a distant, diffuse object is illuminated with spatially coherent radiation, the radiation scattered onto a plane will exhibit the random interference pattern called "speckle." If the plane is located in the far field of the scatterer, then the speckle size is about 1.6 $\lambda\ell/D$, where ℓ is the range and D is the diameter of the scatterer [2]. The speckle area is also equal to the coherence area in the observation plane.

In our case, the far-field distance is hundreds of kilometers from the illuminated patch. However, the speckle size is still approximately that stated above, provided only that many points on the scatterer contribute to the amplitude at any point in the observation plane [3]; this is nearly always the case. We further assume that the coherence area remains equal to the speckle size when in the near field.

We assume the receiver to have a 10-cm-diameter lens. If the receiver is located 10 km from the scatterer, then about 900 speckles fall onto the lens. Because the number is so large, the light may be assumed to be completely incoherent.

Except in the special case where the LED is smaller than the diffraction limit of the collimating lens, the emission from the simulator also is spatially incoherent. Therefore, coherence presents no obstacle to using the LED to simulate the laser return.

Incidentally, the speckle pattern has another effect. The number of bright speckles inside the entrance pupil of the receiver lens is about 450 (half of 900). As a result, the relative fluctuation from shot to shot will

be $1/\sqrt{450}$, or about 5% [4]. Fluctuations with this origin will not exist with the LED source.

Pulse Duration and Shape

The pulse emitted by a Q-switched YAG laser may have a duration from 10 ns to 50 ns or more; often the risetime is substantially shorter than the decay time. We have driven the LEDs with electrical pulses with durations as short as 20 ns and as long as 1 μs. The electrical pulses were symmetric, and the optical pulses were virtually indistinguishable.

The LED manufacturers claim rise and decay times less than 10 ns; this is consistent with our observations. We have made no attempt to determine the ultimate performance of the LEDs.

The LED pulses could, no doubt, be tailored to match the laser pulses, but we cannot foresee any purposes for which this would be desirable. We assume that the receivers would in general be energy detectors; that is, they respond to the energy of the pulse and ignore the waveform. In that case, any LED pulses with the right energy and roughly the right duration would suffice for calibrating receivers. We have easily obtained 20-ns optical pulses, and Franzen and Day in our laboratory have shown how to generate 2.5-ns pulses with similar LEDs [1]. We therefore do not believe that the time-domain properties of the LED pulses will be a hindrance.

Energy Density and Uniformity

Here we address the problem of generating a collimated beam with sufficient intensity and uniformity over a 10-cm diameter. We show in Appendix E that we can expect a total of no more than 10^{-12} J to be collected by the 10-cm objective of the system described in Table 4. We also estimate in that appendix that about that amount of unfiltered energy can be provided by the LEDs with drive currents in excess of 2 A.

To assess the uniformity of the beam across a wide aperture, we roughly collimated the emission from the diodes with a lens whose focal length was about 20 cm and diameter about 10 cm. We pulsed the LEDs and scanned the detector across the aperture of the lens. This procedure does not measure the radiation pattern as a function of angle; for that, we would have to restrict

the detector to a circle centered about the LED. Rather, it measures the more-relevant (for us) irradiance across the exit pupil of the lens.

Figure 8 shows the results of some scans across the F/2 lens. The LEDs that do not use lenses display approximately uniform irradiance across most of the F/2 aperture. The LEDs with the ruby lenses are uniform to ± 5% over about an F/4 aperture.

We also used a uniform large-area silicon detector to measure the approximate power each LED radiated into an F/8 cone. These results are tabulated in Table 6, column 1. We then calculated the approximate power radiated into cones with different F numbers; these calculations are tabulated in the remaining columns of Table 6.

Table 6

Total Energy (10^{-12} J) Radiated Into Various Cones*

	F/8	F/4	F/10	F/20
C30116/F #1	1.5	5.8	0.93	0.23
C30116/F #3	1.4	5.7	0.91	0.23
GAL 100	1.4	5.5	0.88	0.22
GAL 101 #1	1.7	6.7	1.1	0.27
GAL 101 #2	3.1	12.0	2.0	0.50

*For 20-ns pulses, 1-A peak current. To convert to other F numbers, multiply the figures in column 1 by $(8/\text{F number})^2$. To convert to other pulse durations, multiply by (duration/20 ns). To convert to other currents, multiply by (current/1 A).

It is possible to radiate a few times 10^{-12} J into an F/8 cone using any of the LEDs with a drive current of 1 A and a duration of 20 ns. This may be increased by an order of magnitude or more by increasing the current to 10 A and the duration beyond 20 ns.

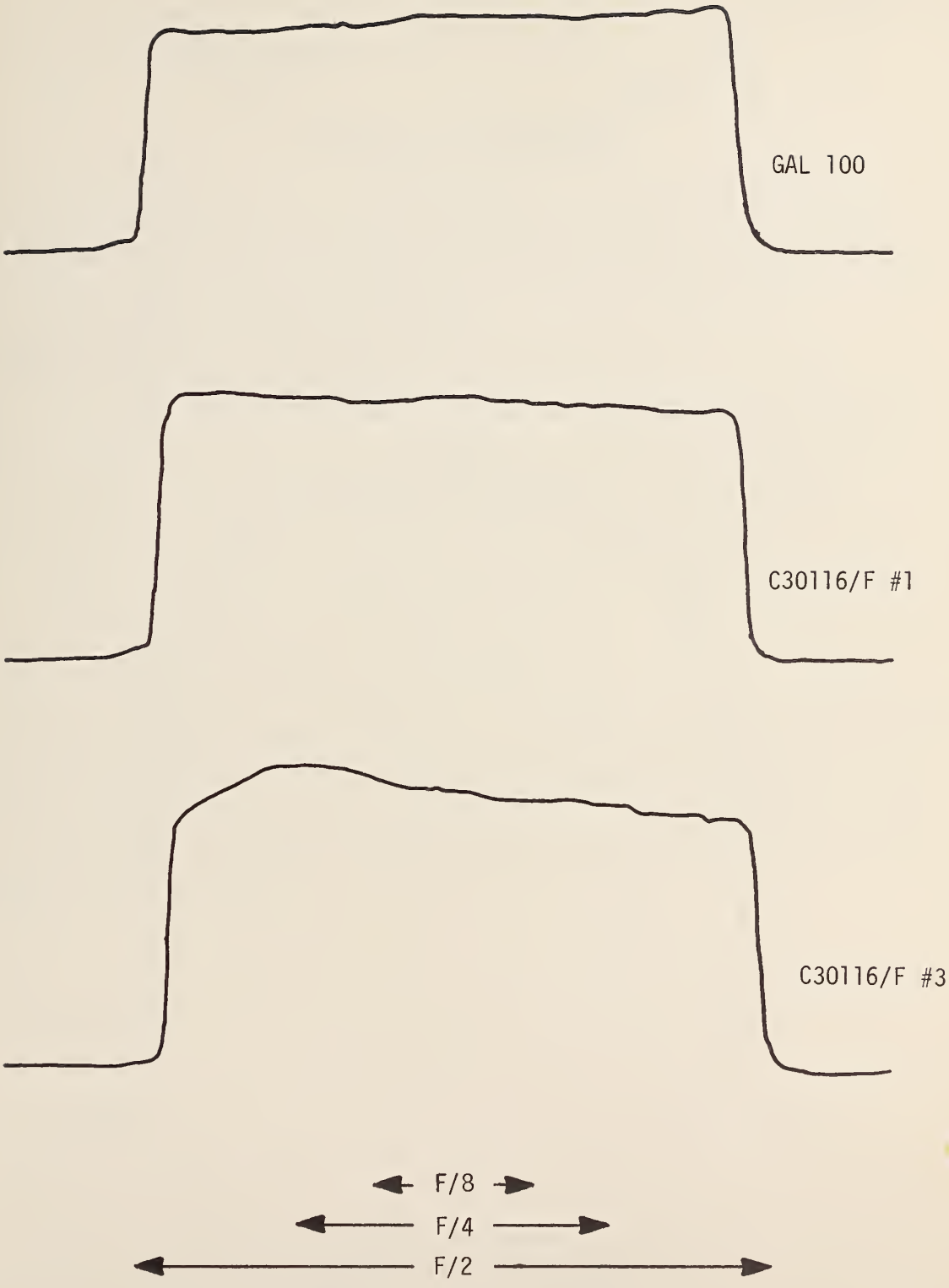

Figure 8a. Exit-pupil scan of three LEDs.

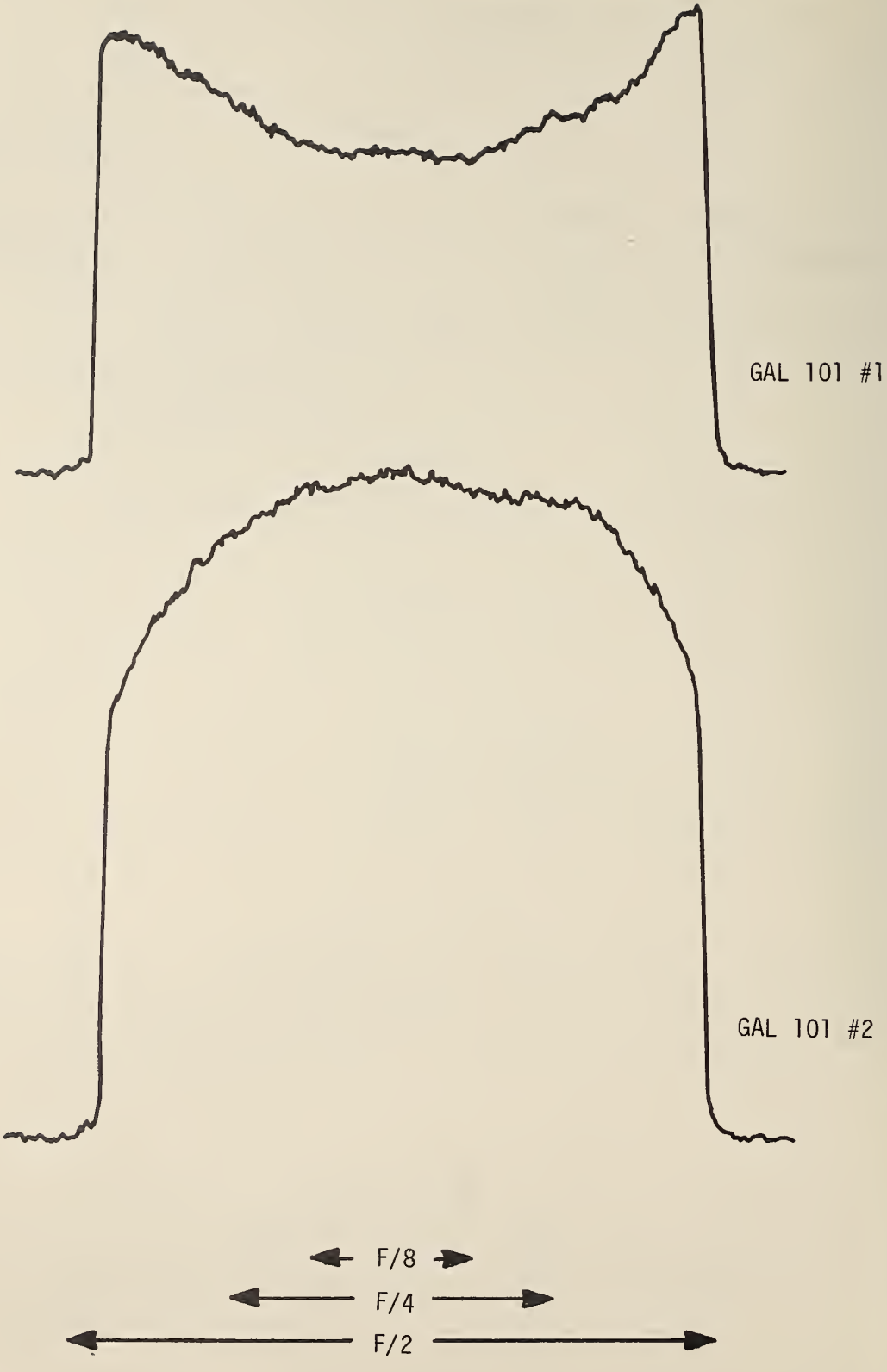

Figure 8b. Exit-pupil scans of two GAL 101s with ruby lenses.

If the receiver system contains a 1-nm filter with its peak at 1064 nm, then the total energy that passes the filter will be at least two orders of magnitude less than the energies listed in Table 6.

Summary and Conclusions

We have shown that there is in principle no reason that an LED may not be used to simulate a diffusely reflected laser beam with certain properties. The most-important practical problem we can foresee is generating sufficient energy per pulse at the right wavelength.

The detailed design of a system is well beyond the scope of this report. However, in such a design, there will likely be compromises made between beam divergence and energy per pulse. For example, if a comparatively large beam divergence may be tolerated, then a relatively low F-number lens may be used to increase the total energy that passes through an aperture with a given diameter. On the other hand, a low beam divergence will require the designer to sacrifice energy by using a low-aperture collimating lens or a spatial filter to reduce the apparent diameter of the source.

Another decision will be whether to (spectrally) filter the LED radiation or to measure the total energy radiated into the lens aperture and to rely on processing to calculate the responsivity of the receiver being tested.

Beyond these, we suspect that the design of a simulator system will be comparatively straightforward if the designer adheres to the principles described in this report.

References

[1] Franzen, D. L., and Day, G. W., LED source for determining optical detector time response at 1.06 μm, Rev. Sci. Instrum. 50, 1029-1031 (1979).

[2] Young, M., Optics and lasers, Springer-Verlag, New York, Heidelberg, Berlin, 1977, Chap. 4.6. Young, M., et al., J. Opt. Soc. Amer. 60, 137-8 (1970).

[3] Dainty, J. C., The statistics of speckle patterns, Sect. 2.1, in Progress in Optics, Vol. XIV, Wolf, E., ed., North-Holland Publishing Co., Amsterdam, New York, Oxford, 1976.

[4] Young, M., and Lawton, R. A., Measurement of pulsed laser power, NBS Technical Note 1010, 1979, Sect. 3.

[5] Ref. 2, Chaps. 1.2 and 2.2.

[6] Ref. 2, equation 1.17.

[7] See, e.g., an article by Smith, W. J. in The Infrared Handbook, Wolfe, W. L. and Zissis, G. J., eds., U.S. Government Printing Office, Washington, 1978; or in Handbook of Optics, Driscoll, W. G., ed., McGraw-Hill Book Company, New York, 1978.

[8] Day, G. W. and Stubenrauch, C. F., Laser far-field beam-profile measurements by the focal plane technique, NBS Technical Note 1001.

[9] Ref. 2, Chap. 3.1.

Appendix A

Effective Transmittance of an Optical Filter

Here we wish to calculate the overall transmittance of a filter when the filter is illuminated by a specific source. We describe the transmittance function of the filter by the function $T(\lambda)$, where T has the maximum value of T_o. The emission spectrum of the source and any additional filters that may be placed in front of the source is described by the function $S(\lambda)$. For mathematical convenience, we normalize S so that

$$\int_0^\infty S(\lambda)\, d\lambda = 1 \ . \tag{A1}$$

The power transmitted by the filter at any wavelength is equal to the product of S and T; therefore, the net (overall) transmittance T_f of the filter is the integral,

$$T_f = \int_0^\infty S(\lambda)\ T(\lambda)\ d\lambda \ . \tag{A2}$$

For exact calculations, the integral must be evaluated digitally after S and T are measured. However, for many purposes, it will suffice to approximate both S and T by Gaussian functions,

$$S(\lambda) = (1/\Delta\lambda_s)\ \exp[-\pi(\lambda-\lambda_s)^2/\Delta\lambda_s{}^2] \tag{A3}$$

and

$$T(\lambda) = T_o\ \exp\ [-\pi(\lambda-\lambda_t)^2/\Delta\lambda_t{}^2], \tag{A4}$$

where $1/\Delta\lambda_s$ is a normalizing factor that satisfies Eq. (A1). The subscripts s and t refer to S and T; λ_s and λ_t are the wavelengths at which S and T are maximum; and $\Delta\lambda$ is the full spectral width at half maximum.

Three cases are important to us. First, assume that S and T are represented by the same function; that is, $\lambda_s = \lambda_t$ and $\Delta\lambda_s = \Delta\lambda_t$. The integral in Eq. (A2) becomes for this case,

$$T_f = (T_o/\Delta\lambda) \int_0^\infty \exp[-2\pi(\lambda-\lambda_o)^2/\Delta\lambda^2]\, d\lambda \ . \qquad (A5)$$

The integral is readily evaluated; Eq. (A5) reduces to

$$T_f = 0.35\ T_o \ . \qquad (A6)$$

When the spectrum of the source and the transmittance of the filter match, the net transmittance of the filter is about one-third the maximum transmittance.

The second case of interest is that for which $\Delta\lambda_t << \Delta\lambda_s$. This approximation will be appropriate when the LED radiation is to be processed with a relatively narrow-band filter. In this case, Eq. (A2) may be written as

$$T_f \cong S(\lambda_t) \int_0^\infty T(\lambda)\, d\lambda \ , \qquad (A7)$$

where $S(\lambda)$ is assumed constant over the region where $T(\lambda)$ is significantly greater than 0. Using the Gaussian approximation again, we find that

$$T_f = S(\lambda_t)\ T_o \Delta\lambda_t \ . \qquad (A8)$$

Equation (A8) may be written in a more convenient form. Let

$$F(\lambda) = S(\lambda)\ \Delta\lambda_s \ . \qquad (A9)$$

$F(\lambda)$ is simply another way of describing the spectrum of the source; when $\lambda = \lambda_s$, $F(\lambda_s)$ is equal to 1. In terms of $F(\lambda)$,

$$T_f = T_o F(\lambda_t)\ \Delta\lambda_t/\Delta\lambda_s \ . \qquad (A10)$$

Finally, when the source spectrum is significantly narrower than the filter transmission spectrum, Eq. (A2) becomes

$$T_f = T(\lambda_s) \int_0^\infty S(\lambda)\, d\lambda \ , \qquad (A11)$$

whence

$$T_f = T(\lambda_s).$$

The three results of this appendix are summarized in Table A1.

Table A1.
Effective Transmittance of Optical Filter

$\Delta\lambda_f < \Delta\lambda_s$	$T_f = T_o F(\lambda_f)\Delta\lambda_f/\Delta\lambda_s$
$\Delta\lambda_o = \Delta\lambda_s$, $\lambda_o = \lambda_s$	$T_f = 0.35\ T_o$
$\Delta\lambda_o > \Delta\lambda_s$	$T = T(\lambda_s)$

Appendix B

Calculation of Acceptable Focus Error

In this appendix, we calculate the precision with which the LED must be located at the focal point of the collimating lens. The calculation is similar to other treatments of depth of focus in photography [5].

Figure B1 shows the collimator and the receiver. For the moment, the LED source is taken to be a point source. The receiver is presumed to have a field stop at the focal point F_2' of the objective lens. The stop restricts the field of view of the instrument to the angle α. The radius of the stop (which may be the detector itself) is therefore $f_2'\alpha/2$. The image is located not at F_2', but at O_2'; the depth of focus of the receiver is δ. Using similar triangles, we calculate that

$$\delta = (f_2')^2\alpha/D, \tag{B1}$$

where $\delta \ll f_2'$. $\pm\ \delta$ is the acceptable amount of focus error of the receiver, provided that the incident radiation is truly collimated.

Using Newton's form of the lens equation, $x\ x' = -\ f'^2$, [5] we may find the nearest object point O_2 whose image will not be vignetted by the stop at F_2'. This is

$$x_2 = -\ D/\alpha\ , \tag{B2}$$

where the minus sign indicates that the point is to the left of the primary focal point of lens 2.

Lens 1 provides a virtual object for lens 2. The virtual object is the image of the source as seen through lens 1. If the virtual object is located at O_2, then its image is projected to O_2'. The system is then on the verge of being out of focus. We wish to calculate the source position x_1 that corresponds to this virtual-object position. For this purpose, we apply Newton's form again, with

$$x_1' = x_2 = -D/\alpha\ . \tag{B3}$$

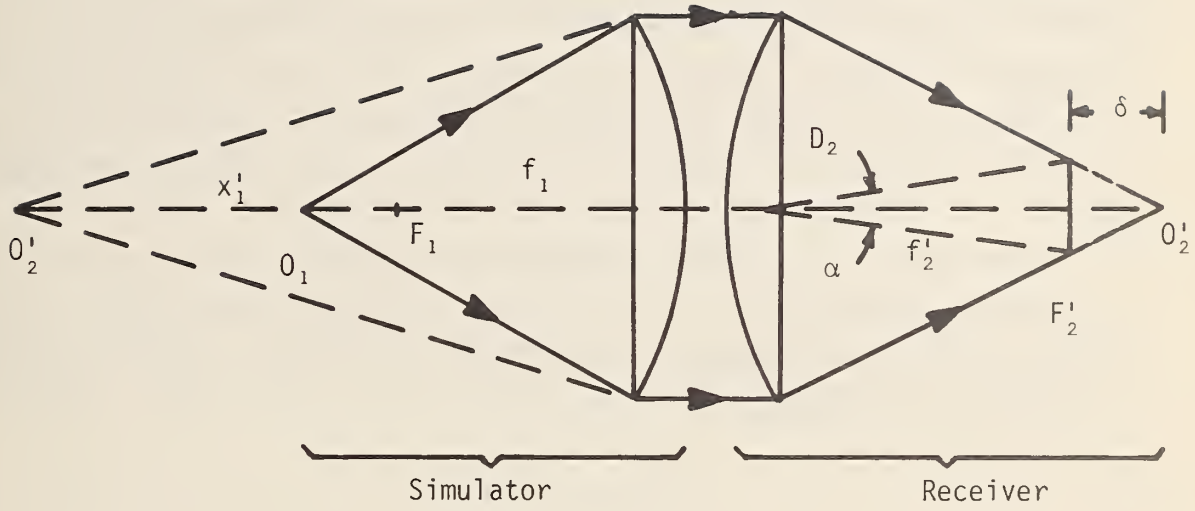

Figure B1. Geometry used for calculating acceptable focus error.

The result,

$$x_1 = - \alpha f_1'^2/D \qquad (B4)$$

indicates the acceptable amount of focus error in the collimating system, presuming that the LED is a point source. Using the parameters relevant to the paradigmatic system of Table 4 (D = 10 cm, α = 0.5 mrad) and assuming that f_2' = 200 cm, we find that the depth of field is 2 cm. The depth of field is very nearly symmetrical about the focal point, so the tolerance is really ± 2 cm.

The source is in reality not a point. With a finite source, the depth of field drops linearly to zero as the angular subtense of the source increases from zero to α. For example, if the source subtends $\alpha/2$, then the depth of field of the collimating lens is ± 1 cm.

Appendix C

Paraxial Optics of a Hemispherical Lens

Figure C1(a) shows a hemispherical lens contacted to a substrate that has a source a distance t behind it. We wish to find the image of this source and the magnification.

To begin, we apply the "len" equation for a single spherical refracting surface [6],

$$(n'/\ell') - (n/\ell) = (n' - n)/R \ . \qquad (C1)$$

The primed symbols refer to the image space, the unprimed symbols to the object space. When n and n' are not equal, the magnification m is given by

$$m = (n/n')\ (\ell'/\ell), \qquad (C2)$$

rather than the customary ℓ'/ℓ.

To locate the image, we first apply Eq. (C1) to the GaAs-ruby interface, for which $R = \infty$. The result, $\ell_1' = -(n'/n)t$, reduces to about t/2 when the appropriate indices are used. (The minus sign indicates that the image is to the left of the interface.) This is the virtual-object point for the ruby-air interface. According to Eq. (C2), the magnification of the image is 1.

We now apply the "len" equation to the second interface, with object distance $\ell_2 = \ell_1'$. The result, $\ell_2' = -\ 432\ \mu m$, locates the virtual image of the original object. The magnification of this stage is $(n/n')\ (\ell'/\ell) \cong 1.8$. The magnification is mainly the result of the fact that the object and image spaces have different indices of refraction and is very nearly the ratio of the indices. As long as t is small compared with R, object and image will lie relatively close together; magnification will vary only slightly with changes of the ratio t/R and will be equal to (n/n') when t=0.

We now ask, How is the on-axis irradiance influenced by the presence of the ruby lens? As Fig. C1(b) suggests, the lens brings about an increase of irradiance as the result of two factors: reduced reflection loss and decreased spreading of the beam refracted at the surface of the GaAs.

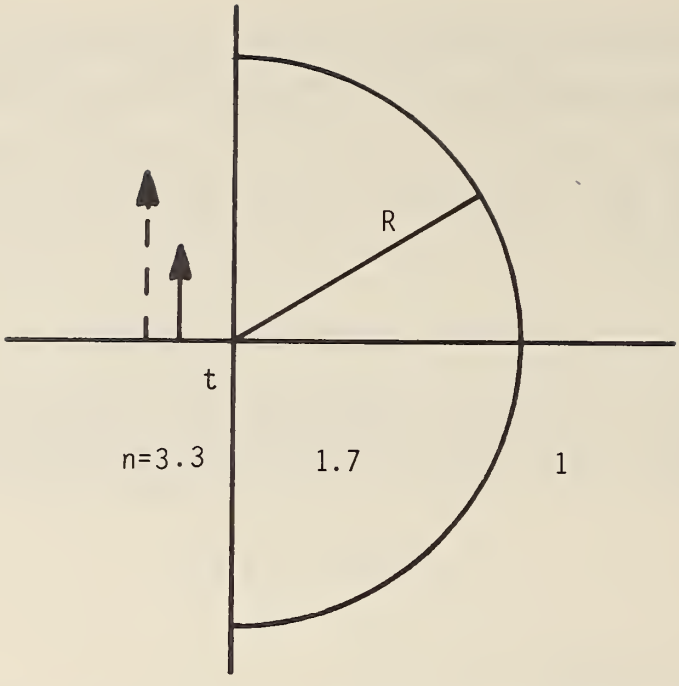

Figure C1a. Hemispherical lens contacted to a substrate with source a depth t inside substrate.

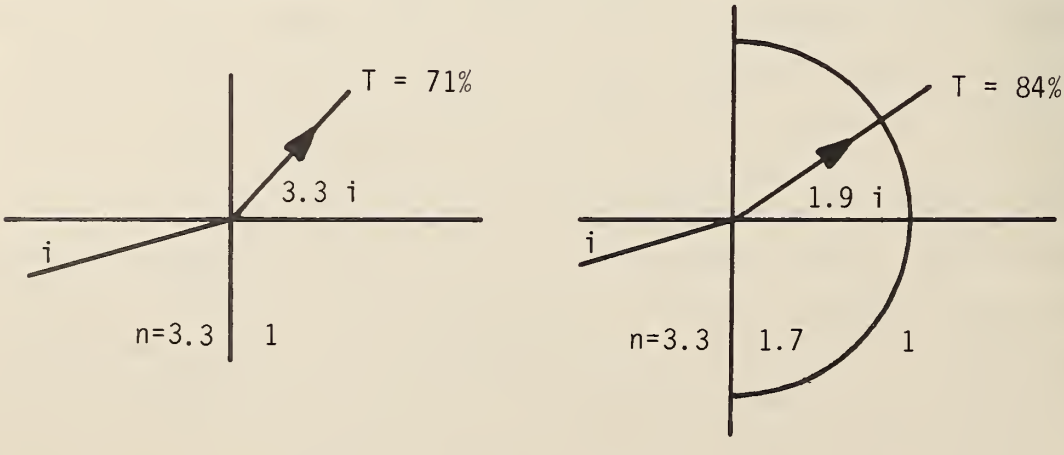

Figure C1b. Refraction by substrate-air interface without (left) and with (right) ruby lens.

Near to normal incidence, the reflectance at an interface is given by the familiar formula,

$$R = (n-1)^2/(n+1)^2 \ ; \qquad (C3)$$

the pertinent indices are 3.3 and 1.7 for GaAs and ruby. The reflectance of a GaAs-air interface is 0.29; the transmittance is therefore 0.71. Consequently, if a ray originates inside the GaAs, only 71% of the power is transmitted across the interface into the air.

Suppose, however, that a ruby lens is contacted very efficiently to the GaAs, as in Fig. C1(b). (We presume that the index of the cement is close to that of the ruby.) Then the transmittances of the two successive interfaces are 0.90 and 0.93; the overall transmittance is 0.84. The gain from reduced reflectance is 0.84/0.71 = 1.18.

Now suppose that a ray crosses the surface of the GaAs with angle of incidence i, which is small. The angle of refraction is 3.3i when the ruby lens is not present, but it is reduced to (3.3/1.7)i when the ruby lens is added. (Because the lens is hemispherical, the angle of incidence at the ruby-air interface is 0.) Thus, a narrow cone directed at the surface of the GaAs is spread into a larger angle when the lens is absent than when it is present. Because of the two-dimensional symmetry, this translates into an increase of irradiance of 1.7^2 as the result of the concentrating effect of the ruby lens.

The total gain resulting from the presence of the lens is the product $1.7^2 \times 1.18$, or about 3.5. This is a power or irradiance gain and not a radiance gain. Because of the magnifying effect of the ruby lens, the increase of source radiance cannot exceed what is gained by reduced reflectance, or about 1.2. If the ruby lens is responsible in some way for the unexpectedly large source diameter noted in the main text, then radiance is actually lost rather than increased.

Appendix D

Aberrations of a Planoconvex Lens

The divergence of the collimated radiation will equal the angular subtense of the LED provided that the aberrations of the lens are kept within certain limits. If space and power are not factors, then the collimator may be a single-element lens with a long focal length and relatively low aperture. (The same is true of the receiver.)

The optimum shape for a positive lens with one conjugate at infinity is nearly planoconvex, with the curved side toward the long conjugate. Because planoconvex lenses are readily available, we limit the discussion to such lenses.

Smith gives relatively complicated formulas for the third-order aberrations of thin lenses when the stop is in contact with the lens [7]. The formulas are written in terms of the refractive index of the glass, the conjugates and the shape of the lens. There is no need to reproduce the formulas here. However, for the special case of a planoconvex lens with one conjugate at infinity, the formulas reduce to comparatively simple form. These are stated in Table D1, in which the transverse aberrations are expressed in units of the Airy-disk radius.

Table D1

Transverse Aberrations of a Planoconvex Lens[1]

Aberration	Formula	Value at 1.06 μm[2]
Spherical	$\frac{0.120\ D}{\lambda(f\#)^3}$	$\frac{1132\ D}{(f\#)^3}$
Coma	$\frac{0.034h}{\lambda(f\#)^3}$	$\frac{321h}{(f\#)^3}$
Astigmatism and field curvature	$\frac{0.205h^2}{\lambda f(f\#)^2}\left(1+\frac{1}{n}\right)$	$\frac{3223h^2}{f(f\#)^2}$

1. In units of $1.22\ \lambda f/D$.
2. All measurements in centimeters. $n = 1.50$.

The transverse aberrations may be used to estimate the size of the image of a distant point; Table D1 refers only to a planoconvex lens with the proper orientation. If the sum of the aberrations in Table D1 is less than 1, then the image size is about equal to the Airy disk size; the image is said to be "diffraction limited." If the sum is greater than 1, then the image is about equal to that many Airy disk radii. (In reality, the semidiameter of the comatic image in the radial direction is 1.5 times the size given by Table D1.) A lens will be acceptable as a collimator provided that the sum of the aberrations is substantially less than the source size required to yield the desired beam divergence.

When the source is precisely on the axis of the lens, then only spherical aberration contributes to the aberration sum; the other aberrations are zero. They are included in the table so that angular tolerance may be calculated as well.

By way of example, let us consider an F/20 lens, focal length 200 cm and diameter 10 cm. Let the source be located 2° off axis; then h is 7 cm (see Fig. D1). Using the formulas in column 3 of Table D1, we find that

$$\text{spherical} = 1.4$$

$$\text{coma} = 0.3$$

and

$$\text{astig.} + \text{f.c.} = 2.0.$$

Using 1.5 times coma for the aberration contribution, we estimate the image semidiameter to be about 4 Airy-disk radii. On the axis, the spherical-aberration contribution is 1.4 Airy disks. This lens is nearly diffraction limited on the axis, but performs somewhat more poorly 2° off the axis. These numbers are in good agreement with a raytrace performed on a similar lens [8].

The beam divergence due to diffraction is $1.22\ \lambda/D$; for this lens, this comes to about 0.01 mrad. At 2° off axis, the beam divergence is less than 0.05 mrad. The lens should be more than adequate to collimate a beam to divergence of 0.5 mrad or less.

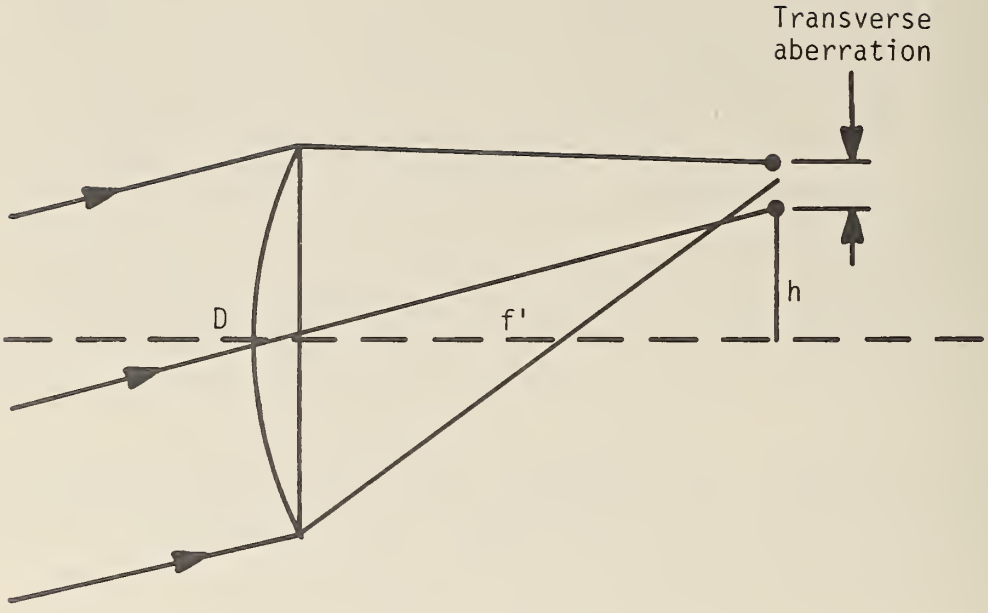

Figure D1. Transverse aberration of a planoconvex lens.

Appendix E

Calculation of Power

Here we make a rough estimate of the power expected to be received at 10-km range by our typical system (Table 4). For the purpose of this calculation, we assume the distant scatterer to be a Lambert diffuser; later, we shall assume the LEDs to be Lambert sources.

The geometry is that of Fig. E1. We assume that all the power emitted by the laser falls onto the diffuser. The fraction of that power that is captured by the receiver may be found from the equation

$$d^2\phi = L\ dS \cos\theta\ d\Omega \tag{E1}$$

where L is the apparent radiance of the scatterer and is given by the relation,

$$L = \phi_0/\pi\ dS\ . \tag{E2}$$

ϕ represents radiant power, dS is the area of the illuminated part of the scatterer, $d\Omega$ is the solid angle subtended by the receiver at the scatterer, and cos θ is 1 for nearly normal incidence [9].

Because the radiation is uniform over the aperture of the receiver, we may set $d\Omega$ equal to the (finite) area of the receiver and implicitly integrate Eq. (E1) with respect to Ω. The result is that

$$d\phi = \phi_0\ D^2/4\ell^2\ . \tag{E3}$$

We are more likely to be interested in energy than in power; therefore, we multiply both sides of Eq. (E3) by time and find that

$$dQ = Q_0 D^2/4\ell^2\ ,$$

where Q represents radiant energy. dQ is the total energy that falls onto the entrance pupil of the receiver, and Q_0 is the energy emitted by the laser.

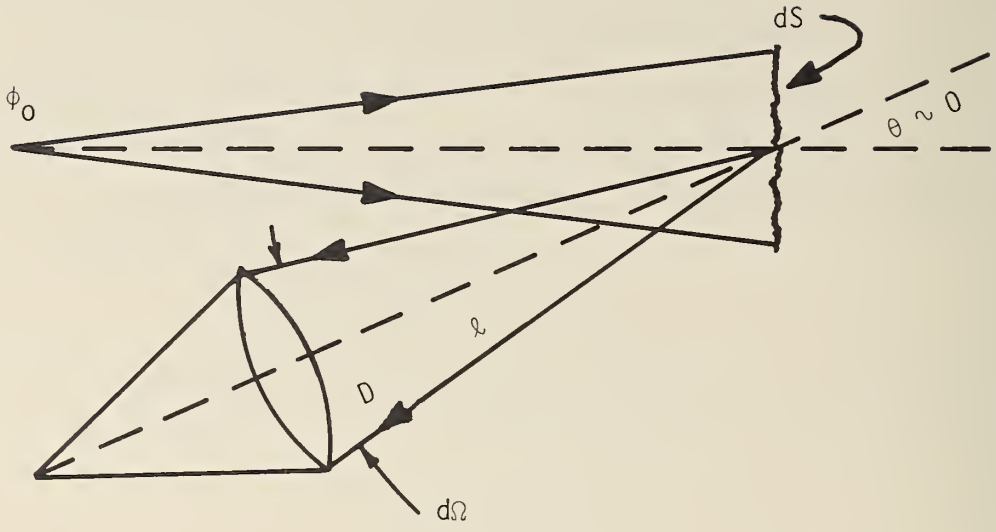

Figure E1. Geometry for determining energy collected by receiver.

Appendix F

Angular Tolerance of Interference Filter

We assume that the interference filters are the metal-dielectric-metal or Fabry-Perot type. The wavelength of maximum transmittance is given by the equation,

$$m\lambda = 2d \ . \tag{F1}$$

If the filter is tilted slightly, Eq. (E1) becomes

$$m\lambda' = 2d \cos \theta \ , \tag{F2}$$

where λ' is the wavelength of the maximum at the angle θ. If λ' differs from λ by substantially less than the passband of the filter, then the tilt is inconsequential.

We calculate the difference $\delta\lambda$ between λ' and λ by assuming that θ is relatively small and approximating the cosine by the first two terms in its Maclaurin expansion,

$$\cos \theta \cong 1 - \theta^2/2, \tag{F3}$$

whence,

$$\delta\lambda/\lambda = - \theta^2/2 \ . \tag{F4}$$

If we demand that $\delta\lambda$ be less than the half width $\Delta\lambda/2$ of the filter, we find that

$$\theta^2 < \Delta\lambda/\lambda \ . \tag{F5}$$

The passband of the filter of Table 4 is 100 nm and the maximum about 1000 nm. Thus, Eq. (F5) shows that the transmission band will shift appreciably only if θ is about 20° or more. Let us therefore say that the angular tolerance of the filter is about 4°. This is approximately the vertex angle

If Q_0 = 0.1 J, D = 10 cm and ℓ = 10 km, then dQ is about 2.5 x 10^{-12} J. Allowing for loss (such as diffuser reflectance's being less than 1), we may say that the total energy collected by the receiver will be as small as 10^{-12} J or less.

Next, we estimate the energy transmitted from the LED through the lens. If the LED may be regarded as a Lambert soure, then the power $\phi(\theta)$ radiated into a cone with vertex angle θ is

$$\phi(\theta) = \phi_0 \sin^2\theta \ , \tag{E4}$$

where ϕ_0 is the power radiated into a hemisphere [9]. Using the relation that

$$\sin\theta \cong D/2f' = 1/2f\# \ , \tag{E5}$$

we may write $\phi(\theta)$ in the form

$$\phi(\theta) \cong \phi_0/(2f\#)^2 \ . \tag{E6}$$

If ϕ_0 represents the peak power of a pulse whose duration is τ, then

$$Q(\theta) = \phi_0 \tau/(2f\#)^2 \ , \tag{E7}$$

where Q is radiant energy.

If the peak power of the pulses is 4 mW (corresponding to 2-A drive current in some LEDs) and the duration is 40 ns, then we may expect 10^{-13} J into an F/20 aperture. (If the radiation is filtered, then the energy may be an order of magnitude less.) In fact, certain LEDs are manufactured with a condensing lens in close contact, so the power at normal incidence may be substantially greater than that predicted for a Lambert source. Actual measurements, including the uniformity of the radiation pattern across the lens aperture, have been left to the experimental sections in the body of the report.

of an F/8 cone. Therefore, the filter may be placed into an F/8 cone without harmful effects. Cones with higher relative aperture than F/8 may be dangerous; in such cases, optics will have to be provided to place the filter in a more-nearly collimated beam.

NBS-114A (REV. 9-78)

U.S. DEPT. OF COMM. BIBLIOGRAPHIC DATA SHEET	1. PUBLICATION OR REPORT NO. NBS TN-1031	2. Gov't. Accession No.	3. Recipient's Accession No.

4. TITLE AND SUBTITLE

The Use of LEDs to Simulate Weak YAG-Laser Beams

5. Publication Date: January 1981

6. Performing Organization Code

7. AUTHOR(S)

Matt Young

8. Performing Organ. Report No.

9. PERFORMING ORGANIZATION NAME AND ADDRESS

NATIONAL BUREAU OF STANDARDS
DEPARTMENT OF COMMERCE
WASHINGTON, DC 20234

10. Project/Task/Work Unit No.

11. Contract/Grant No.

12. SPONSORING ORGANIZATION NAME AND COMPLETE ADDRESS *(Street, City, State, ZIP)*

Mr. Barry Hardin
ASD/AER-EA,
Wright-Patterson Air Force Base, Ohio 45433

13. Type of Report & Period Covered

14. Sponsoring Agency Code

15. SUPPLEMENTARY NOTES

☐ Document describes a computer program; SF-185, FIPS Software Summary, is attached.

16. ABSTRACT *(A 200-word or less factual summary of most significant information. If document includes a significant bibliography or literature survey, mention it here.)*

The purpose of this report is to determine whether and under what conditions a light-emitting diode may be used to simulate a weak YAG-laser beam that has been scattered by a distant reflecting object. By examining the differences between laser radiation and LED radiation, we conclude that there is no theoretical reason that a LED may not be used in place of the laser beam.

17. KEY WORDS *(six to twelve entries; alphabetical order; capitalize only the first letter of the first key word unless a proper name; separated by semicolons)*

Laser simulator; light-emitting diodes; YAG laser

18. AVAILABILITY ☒ Unlimited

☐ For Official Distribution. Do Not Release to NTIS

☒ Order From Sup. of Doc., U.S. Government Printing Office, Washington, DC 20402,

☐ Order From National Technical Information Service (NTIS), Springfield, VA, 22161

19. SECURITY CLASS (THIS REPORT): UNCLASSIFIED

21. NO. OF PRINTED PAGES: 48

20. SECURITY CLASS (THIS PAGE): UNCLASSIFIED

22. Price: $2.50

NBS TECHNICAL PUBLICATIONS

PERIODICALS

JOURNAL OF RESEARCH—The Journal of Research of the National Bureau of Standards reports NBS research and development in those disciplines of the physical and engineering sciences in which the Bureau is active. These include physics, chemistry, engineering, mathematics, and computer sciences. Papers cover a broad range of subjects, with major emphasis on measurement methodology and the basic technology underlying standardization. Also included from time to time are survey articles on topics closely related to the Bureau's technical and scientific programs. As a special service to subscribers each issue contains complete citations to all recent Bureau publications in both NBS and non-NBS media. Issued six times a year. Annual subscription: domestic $13; foreign $16.25. Single copy, $3 domestic; $3.75 foreign.

NOTE: The Journal was formerly published in two sections: Section A "Physics and Chemistry" and Section B "Mathematical Sciences."

DIMENSIONS/NBS—This monthly magazine is published to inform scientists, engineers, business and industry leaders, teachers, students, and consumers of the latest advances in science and technology, with primary emphasis on work at NBS. The magazine highlights and reviews such issues as energy research, fire protection, building technology, metric conversion, pollution abatement, health and safety, and consumer product performance. In addition, it reports the results of Bureau programs in measurement standards and techniques, properties of matter and materials, engineering standards and services, instrumentation, and automatic data processing. Annual subscription: domestic $11; foreign $13.75.

NONPERIODICALS

Monographs—Major contributions to the technical literature on various subjects related to the Bureau's scientific and technical activities.

Handbooks—Recommended codes of engineering and industrial practice (including safety codes) developed in cooperation with interested industries, professional organizations, and regulatory bodies.

Special Publications—Include proceedings of conferences sponsored by NBS, NBS annual reports, and other special publications appropriate to this grouping such as wall charts, pocket cards, and bibliographies.

Applied Mathematics Series—Mathematical tables, manuals, and studies of special interest to physicists, engineers, chemists, biologists, mathematicians, computer programmers, and others engaged in scientific and technical work.

National Standard Reference Data Series—Provides quantitative data on the physical and chemical properties of materials, compiled from the world's literature and critically evaluated. Developed under a worldwide program coordinated by NBS under the authority of the National Standard Data Act (Public Law 90-396).

NOTE: The principal publication outlet for the foregoing data is the Journal of Physical and Chemical Reference Data (JPCRD) published quarterly for NBS by the American Chemical Society (ACS) and the American Institute of Physics (AIP). Subscriptions, reprints, and supplements available from ACS, 1155 Sixteenth St., NW, Washington, DC 20056.

Building Science Series—Disseminates technical information developed at the Bureau on building materials, components, systems, and whole structures. The series presents research results, test methods, and performance criteria related to the structural and environmental functions and the durability and safety characteristics of building elements and systems.

Technical Notes—Studies or reports which are complete in themselves but restrictive in their treatment of a subject. Analogous to monographs but not so comprehensive in scope or definitive in treatment of the subject area. Often serve as a vehicle for final reports of work performed at NBS under the sponsorship of other government agencies.

Voluntary Product Standards—Developed under procedures published by the Department of Commerce in Part 10, Title 15, of the Code of Federal Regulations. The standards establish nationally recognized requirements for products, and provide all concerned interests with a basis for common understanding of the characteristics of the products. NBS administers this program as a supplement to the activities of the private sector standardizing organizations.

Consumer Information Series—Practical information, based on NBS research and experience, covering areas of interest to the consumer. Easily understandable language and illustrations provide useful background knowledge for shopping in today's technological marketplace.

Order the **above** *NBS publications from: Superintendent of Documents, Government Printing Office, Washington, DC 20402.*

Order the **following** *NBS publications—FIPS and NBSIR's—from the National Technical Information Services, Springfield, VA 22161.*

Federal Information Processing Standards Publications (FIPS PUB)—Publications in this series collectively constitute the Federal Information Processing Standards Register. The Register serves as the official source of information in the Federal Government regarding standards issued by NBS pursuant to the Federal Property and Administrative Services Act of 1949 as amended, Public Law 89-306 (79 Stat. 1127), and as implemented by Executive Order 11717 (38 FR 12315, dated May 11, 1973) and Part 6 of Title 15 CFR (Code of Federal Regulations).

NBS Interagency Reports (NBSIR)—A special series of interim or final reports on work performed by NBS for outside sponsors (both government and non-government). In general, initial distribution is handled by the sponsor; public distribution is by the National Technical Information Services, Springfield, VA 22161, in paper copy or microfiche form.

U.S. DEPARTMENT OF COMMERCE
National Bureau of Standards
Washington, D.C. 20234

OFFICIAL BUSINESS

Penalty for Private Use, $300

POSTAGE AND FEES PAID
U.S. DEPARTMENT OF COMMERCE
COM-215

SPECIAL FOURTH-CLASS RATE
BOOK